



OPEN ACCESS

EDITED BY
Zhonghua Gou,
Wuhan University, China

REVIEWED BY
Xin-Chen Hong,
Fuzhou University, China
Zhikang Bao,
City University of Hong Kong,
Hong Kong SAR, China

*CORRESPONDENCE
Tiejun Zhou
zhoujt777@163.com

SPECIALTY SECTION
This article was submitted to
Environmental Health and Exposome,
a section of the journal
Frontiers in Public Health

RECEIVED 04 August 2022
ACCEPTED 30 August 2022
PUBLISHED 04 November 2022

CITATION
Wang Y, He B-J, Kang C, Yan L,
Chen X, Yin M, Liu X and Zhou T (2022)
Assessment of walkability and walkable
routes of a 15-min city for heat
adaptation: Development of a dynamic
attenuation model of heat stress.
Front. Public Health 10:1011391.
doi: 10.3389/fpubh.2022.1011391

COPYRIGHT
© 2022 Wang, He, Kang, Yan, Chen,
Yin, Liu and Zhou. This is an
open-access article distributed under
the terms of the [Creative Commons
Attribution License \(CC BY\)](https://creativecommons.org/licenses/by/4.0/). The use,
distribution or reproduction in other
forums is permitted, provided the
original author(s) and the copyright
owner(s) are credited and that the
original publication in this journal is
cited, in accordance with accepted
academic practice. No use, distribution
or reproduction is permitted which
does not comply with these terms.

Assessment of walkability and walkable routes of a 15-min city for heat adaptation: Development of a dynamic attenuation model of heat stress

Yu Wang¹, Bao-Jie He^{1,2,3,4}, Chong Kang⁵, Li Yan⁵,
Xueke Chen¹, Mingqiang Yin¹, Xiao Liu^{4,6,7} and Tiejun Zhou^{1,3*}

¹School of Architecture and Urban Planning, Chongqing University, Chongqing, China, ²Institute for Smart City of Chongqing University in Liyang, Chongqing University, Liyang, China, ³Key Laboratory of New Technology for Construction of Cities in Mountain Area, Ministry of Education, Chongqing University, Chongqing, China, ⁴State Key Laboratory of Subtropical Building Science, South China University of Technology, Guangzhou, China, ⁵School of Civil Engineering and Architecture, Southwest University of Science and Technology, Mianyang, China, ⁶School of Architecture, South China University of Technology, Guangzhou, China, ⁷Architectural Design and Research Institute Co., Ltd., South China University of Technology, Guangzhou, China

Actively addressing urban heat challenges is an urgent task for numerous cities. Existing studies have primarily developed heat mitigation strategies and analyzed their cooling performance, while the adaptation strategies are far from comprehensive to protect citizens from heat-related illnesses and deaths. To address this research gap, this paper aims to enhance people's adaptation capacity by investigating walkability within fifteen-minute cities (FMC). Taking cognizance of thermal comfort, health, and safety, this paper developed a dynamic attenuation model (DAM) of heat stress, along with heat stress aggravation, continuance, and alleviation. An indicator of remaining tolerant heat discomfort (R_t) was proposed with the integration of the Universal Thermal Climate Index (UTCI) to assess heat-related walkability. Following an empirical study among 128 residents in Mianyang, China, and assessing four levels of heat stress, the maximum tolerant heat discomfort was determined to be 60 min. Furthermore, the DAM was applied to an FMC with 12 neighborhoods in Fucheng, Mianyang, China. The results indicate that for each neighborhood, the street was generally walkable with an R_t ranging between 15 and 30 min, after walking for 900 m. A population-based FMC walkability was further determined, finding that the core area of the FMC was favorable for walking with an R_t of 45–46 min, and the perpetual areas were also walkable with an R_t of 15–30 min. Based on these results, suggestions on the frequency of public services (frequently used, often used, and occasionally used) planning were presented. Overall, this paper provides a theoretical model for analyzing walkability and outlines meaningful implications for planning heat adaptation in resilient, safe, comfortable, and livable FMCs.

KEYWORDS

extreme heat, 15-min city, thermal comfort, dynamic attenuation model, UTCI, ENVI-met

Introduction

Cities are now the main human settlement and urbanization will remain mainstream in the coming decades, especially in Asian and African nations (1). Whilst urban living infrastructure is getting better and living quality is improving, the upward trend of urbanization is accompanied by various challenges such as climate change, environmental deterioration, traffic congestion, housing shortage, urban noise, rapid economic development, and inadequate health facilities (2–4). To address such challenges, the UN Sustainable Development Goals (SDGs), particularly Goal 11, suggested the creation of sustainable cities and communities to ensure cities are inclusive, safe, resilient, and sustainable. Goal 11 is interconnected with other goals such as Goal 13 on climate action, where changing climate is a macro driver of various disasters such as urban flooding, extreme heat, and air pollution. Problems such as urban flooding and air pollution have already been widely recognized, and various interventions and actions in aspects of policy, finance, programs, and initiatives have been implemented to address them. However, urban heat challenges have not received enough attention from society and limited measures have been adopted in practice (5).

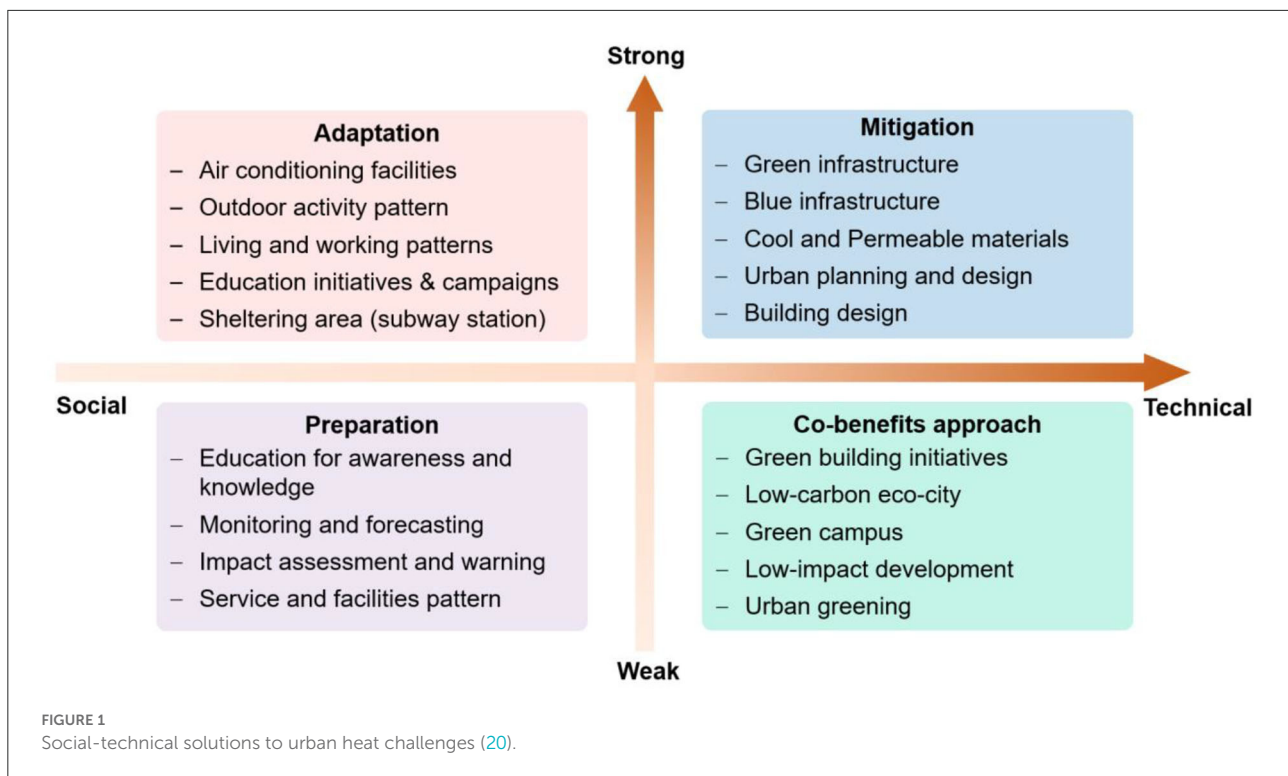
Urban heat is the combined effect of heat waves and urban heat islands (UHIs) associated with climate change and urbanization (6). Numerous climate-related research among urban physicists and meteorologists have revealed the formation, aggravation, and drivers of urban heat (7–9). Their significant impact on environmental, economic, social, and health aspects has also been widely reported (10). However, urban heat has not been widely recognized as an emergent disaster, although it has caused excessive deaths (11–13). The extreme heat event in August 2003 killed more than 70,000 Europeans (14). In 2015, about 3,000 French lost their lives because of extreme heat events (15). In 2019 and 2020, the extreme heat killed 2,000 people each year in England (16). Urban heat has now emerged as a silent killer, causing higher mortality than any other climate-related disaster (17). In the coming decades, heat waves are projected to be more frequent, intense, and longer. While at the same time, contiguous modifications of natural environments during urbanization will further aggravate UHIs in dense and prominent areas associated with heat-absorption and storage material use, nature-based infrastructure reduction, anthropogenic heat release, and increased urban density (18). Synergies between heat waves and UHIs can possibly further aggravate heat-induced impacts (19). In general, addressing the urban heat challenge is an urgent task, not only for the current situation but also in the context of constant climate change.

To address heat-related challenges, He et al. (20) developed a comprehensive heat-resilient framework consisting of heat preparation, heat mitigation, heat adaptation, and a co-benefits

approach (20). Heat preparation refers to the development of heat monitoring, impact assessment, heat health information transfer, and education system to improve heat impact prediction capability and to increase people's awareness and knowledge of what heat impacts are and how to address them. Heat mitigation is focused on heating source dissipation and cooling source enhancement through green and blue infrastructure (21, 22), innovative materials (reflective, retro-reflective, and permeable) (23, 24), urban ventilation (25, 26), and shading structures (27, 28) (Figure 1). Although heat adaptation does not alleviate heat severity from the source, it is currently the most effective approach to protecting people from heat-related illnesses and deaths through the adoption of air-conditioning facilities, behavioral and operational change, and activity rescheduling. The co-benefits approach has been thought of as a win-win strategy in tackling climate change issues by employing the additional benefits of other projects and initiatives for heat preparation, mitigation, and adaptation (29).

Heat adaptation is complex depending on individuals' body heat tolerance, personal behaviors, enterprise operation, and governmental department adaptation. First, the body can resist heat stresses to an extent, which is also known as body thermoregulation. The heat resistance capacity varies with demographic characteristics (such as gender, health, and age), where children and older adults are weak in resisting heat stresses (30). Second, people can change their daily functions such as outdoor activities, work/study, transportation, sleep/rest, and diet in types, time, and duration to adapt to heat (31). In particular, laborers and farmers who need to work outdoors can take their breaks in air-conditioned places or cooling centers during extremely hot temperatures (32). People can select heat-resilient walking routes if outdoor activities are necessary (33). Third, enterprises could upgrade service or operation patterns to ensure emergency systems and public facilities work well under extreme conditions (34). For instance, electricity suppliers could improve production and upgrade the grid to meet increasing energy demands associated with the increase in air-conditioning systems for cooling and overcome grid failure due to extreme heat (34). Fourth, governmental departments could improve their responses for dealing with urban heat by recognizing challenges, formulating policies, setting up financial schemes, and supporting pilot projects and initiatives, to overcome the lack of policies and formal governance (35). However, knowledge of how to improve heat resilience capacity in these four aspects is still a big research gap.

Many global cities are exploring 15-minute city (FMC) models aiming to promote the creation of sustainable and livable communities, neighborhoods, and 15-minute community-life circles with three primary goals of inclusion, health, and safety (36). The FMC initiative is an active response to SDG 11 on sustainable cities and communities to make cities and communities inclusive, safe, resilient, and sustainable. Various



FMC frameworks have been piloted in cities across the world including Australia, China, Colombia, France, Italy, and the United States (36). Whilst such frameworks consider factors such as residence, job opportunities, transport, services, and entertainment, the improvement of heat resilience capacity has not been considered, or at least the interlinkage between FMC and extreme heat, a macro background of numerous cities, has not been well considered. It is essential to integrate heat resilience into FMC planning. Until now, the only work on the integration of heat resilience and FMC has been conducted by Chen and He (37) by developing a framework to integrate heat adaptation into FMC through the identification of heat impacts, recognition of heat-induced impact, documentation of influential factors, the suggestion of heat adaptation strategies, and optimization of adaptation (37).

To overcome the research gap relevant to heat resilience and its integration into FMC, this paper aims to investigate the heat-related walkability within the FMC. The consideration of heat impacts on walkability adds new knowledge to people's understanding of neighborhood walkability based on facilities, public services, and demographic characteristics (38, 39). In particular, this paper developed a dynamic attenuation model (DAM) of heat stress to assess heat tolerance when people are walking along specific routes. The model was further applied to an FMC in Fucheng District, Mianyang, China, to identify the heat stresses and

the most walkable paths. Overall, this paper can better support stakeholders to integrate heat resilience into FMC and improves the understanding of walkability amid heat stresses.

Heat-related adaptation and heat tolerance

Based on the three primary goals of inclusion, health, and safety in the FMC, the targets of heat resilience improvement are expected to be inclusion, health, and safety. Namely, the fundamental target of integrating heat resilience into FMC is to improve all possible individuals' capacity of avoiding heat-related impacts on thermal comfort, heat stresses, illnesses, and deaths through heat preparation, mitigation, and adaptation. Beyond this, the integration can further enhance economic growth and social equality by improving thermal environments. There have been numerous indicators to assess the thermal conditions of outdoor environments, such as air temperature, surface temperature, heat stress, and thermal comfort. Among them, thermal comfort, which refers to individuals' subjective feelings of thermal environments, has been widely accepted to assess if the environment is suitable for activities such as working, walking, and standing.

Thermal comfort and assessment indicators

Subjective feelings are the combination of physical, physiological, and psychological responses to thermal environments (40). The psychological response is associated with people's experience and expectations during the perception and reaction toward heat senses. The physiological response is assessed by the thermo-adaptive approach and governed by the human heat balance, under the change of physical heat exposure. The physiological responses can be measured by the body core temperature, sweat rate, and skin temperature (41). The physical response is relevant to the built form and microclimatic environments which can affect the individuals' physiological responses. Many recent studies have linked physical environments in terms of sound and visual landscape with psychological responses (41). In addition, thermal comfort can be regulated by social and behavioral characteristics (42, 43).

Studies on thermal comfort have been conducted for over 100 years, and the PMV-PPD was the first thermal comfort evaluation indicator developed by Fanger to define comfort, by considering heat-balance equations and empirical studies about skin temperature. It presents a simple method of a seven-point scale from cold (−3) to hot (+3) to survey respondents' feelings (44). Following Fanger, more than 160 thermal comfort assessment indicators have been proposed (45). The WetBulb Globe Temperature (WBGT) is a comprehensive temperature index to evaluate the impacts of temperature, humidity, and solar radiation on people (45). In general, the larger the WBGT value, the harder it is for the human sweat to evaporate, and the lower the body's ability to dissipate heat. This indicator has been used to inform industrial hygienists, athletes, sporting events, and the military of suitable situations for exercise. For instance, during hot climates in the US, when the WBGT is below 22°C, individuals can conduct normal activities, and when the WBGT increases to 28.8°C, there should be limited intense exercises and total daily exposure to heat and humidity. When the WBGT increases to 31.0°C, all exercises should be canceled (46).

The physiological equivalent temperature (PET) and the Universal Thermal Climate Index (UTCI) are found to be the most accurate indicators of outdoor thermal comfort assessment. Both PET and UTCI are a function of environmental parameters (e.g., air temperature, relative humidity, wind speed, solar radiation) and personal behaviors (e.g., clothing, metabolic rate). Both have been classified into different grades of heat stress according to different values (Table 1). For instance, a PET value ranging between 35 and 41°C indicates strong heat stress for western/middle European countries (47). However, there are some differences in people's feelings toward heat stresses after long-term adaptation, where a PET ranging between 38 and 42°C indicates strong heat stress for people from subtropical areas (48). In comparison, the UTCI has different levels of heat

stress, where a UTCI value ranging from 38 to 46°C indicates a very strong heat stress (49). Both PET and UTCI have a significant correlation with extreme heat-induced mortality. For example, Matzarakis et al. (47) analyzed the relationship between heat stress and mortality from 1970 to 2007, finding that in Vienna, at 14:00 central Europe time, the mortality at a PET value of 41°C increased to 8.9% on the first day and reached the maximum value of 27.4% on the fourth day, about 3.42 and 10.53 times, respectively of the average mortality level (2.6%) (47). Furthermore, by analyzing the relationship between daily mortality and heat stress in eight Polish cities between 1975 and 2014, Kuchcik found that the risk of death increased to 10–20% in most cities when the UTCI exceeded 32°C, and to 25–30% when the UTCI crossed 38°C (50).

Spatiotemporal heterogeneity of thermal environments

Heat intensity of outdoor environments is determined by heat sinks and sources which are always highly heterogeneous spatially and temporally. Open spaces such as streets, squares, plazas, grassland, and park for people's outdoor activities, generally exhibit differences in land cover (e.g., pavement, vegetation, water bodies) (51, 52), and surface structure (such as building height, street width, orientation, and density) (53, 54), resulting in the heterogeneity of microclimatic conditions and human thermal comfort. For instance, a square paved with cool materials could be 12°C cooler in surface temperature and 1.9°C cooler in peak air temperature (55). A study in Taipei indicated that parks could generate an average airborne cooling effect of 0.81°C in summer noon, and a cooling effect of 0.29 °C in summer night (56). Water bodies could be strong cooling sinks, compared with many other land use types (e.g. vegetation, road, building, bare land) (57). Overall, the heterogeneity of thermal environments generates significant implications for outdoor activities, transport, and heat health issues (58).

Existing studies have extensively reported the spatial heterogeneity of microclimates and outdoor thermal comfort. For instance, at the building scale, a study in Tianjin, China, indicated that daily maximum temperature decreased with building height at an average rate of 0.05°C for every 10 meters (59). However, the daily minimum temperature increased with building height at an average rate of 0.08°C for every 10 m. At the street scale, street orientation, aspect ratio, length-width ratio, sky view factor, enclosure degree, and building elevation can regulate aerodynamic and radiation properties and thereby the variation of thermal characteristics. A study conducted by Emmanuel et al. (60) in Colombo, Sri Lanka, found that air temperature reduced proportionally with the street aspect ratio and the distance from the sea, and the wind speed increased with the street aspect ratio (60). Street orientation affects solar

TABLE 1 Heat stress and thermal comfort indicators of PET and UTCI (47–49).

| Stress category | PET range for Western/Middle European countries (°C) | PET range for subtropical regions (°C) | UTCI range (°C) |
|-------------------------|--|--|-----------------|
| Extreme cold stress | <-4 | <14 | <-40 |
| Very strong cold stress | - | - | -40 to -27 |
| Strong cold stress | 4–8 | 14–18 | -27 to -13 |
| Moderate cold stress | 8–13 | 14–22 | -13 to -0 |
| Slight cold stress | 13–18 | 22–26 | 0–9 |
| No thermal stress | 18–23 | 26–30 | 9–26 |
| Slight heat stress | 23–29 | 30–34 | - |
| Moderate heat stress | 29–35 | 34–38 | 26–32 |
| Strong heat stress | 35–41 | 38–42 | 32–38 |
| Very strong heat stress | - | - | 38–46 |
| Extreme heat stress | >41 | >42 | >46 |

radiation incidence. Ali Toudert and Mayer found that east-west streets were exposed to direct solar radiation much longer than other streets so thermal environments and thermal comfort in east-west streets were much worse (61). Taleghani et al. (62) analyzed summertime street thermal environments of a Netherland neighborhood, finding that east-west streets could receive solar radiation for 12.5 h, much longer than north-south streets (4.5 h). Moreover, the higher the sky view factor, the higher the mean radiant temperature (62). At the precinct scale, the thermal environments could be more complex due to the combined effects of building height, street structure, and building density. According to the local climate zone studies, the industrial and compact high-rise precincts could be much warmer than all other types. According to the precinct ventilation zone, open low-rise precincts in Sydney were the worst in PET, followed by open midrise and compact high-rise precincts (26).

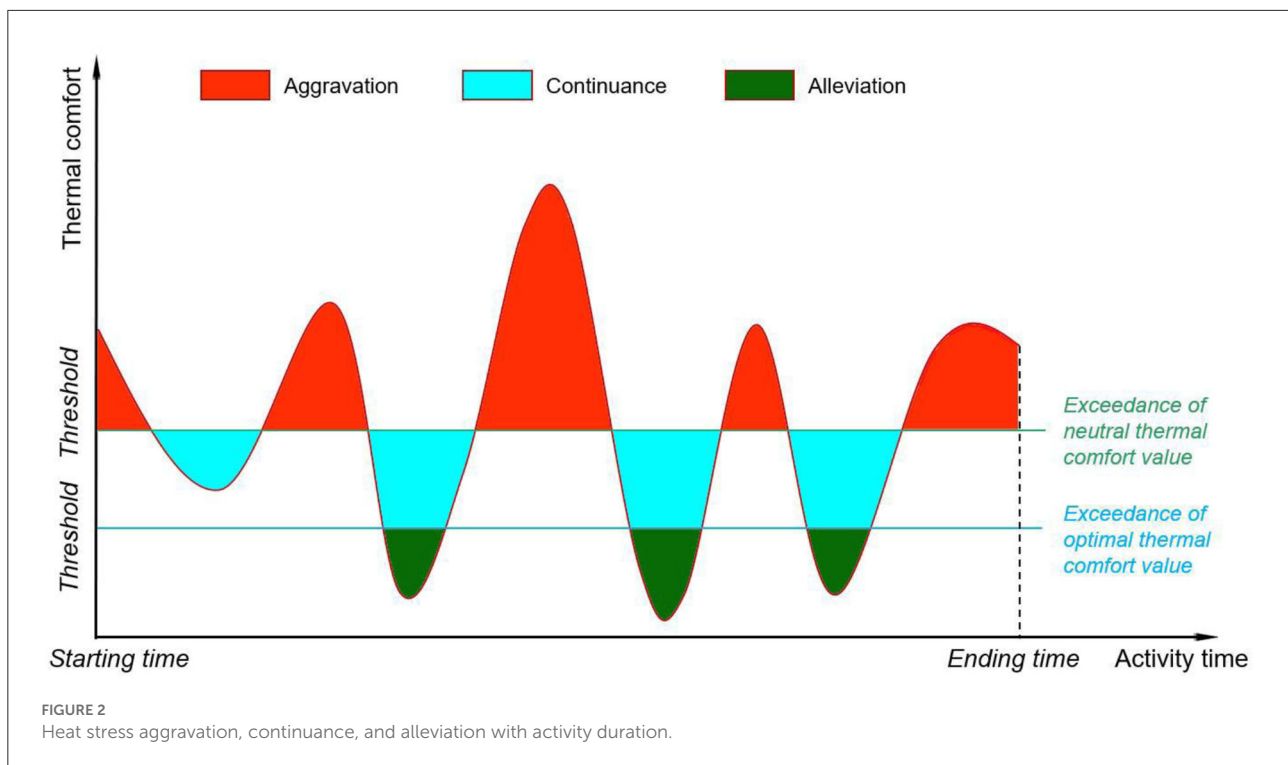
Shading structures or tree shade could also result in strong cooling performance in the mean radiant temperature reduction (63, 64). Trees, in particular, could generate shades and evapotranspiration effects for better cooling performance. Existing studies indicate that though different tree species could have different cooling effects, the ambient temperature could still reduce by 0.5–1.0°C, and the reduction of mean radiant temperature was more prominent by 10°C (65). Local adoption of tree cooling strategies could increase the heterogeneity of street thermal environments since trees are not planted evenly in numerous precincts. In addition, waste heat or cold sources released from air-conditioning systems, traffic systems, and open doors and windows in and surrounding public spaces can also cause significant changes in local microclimate and thermal comfort (9). Overall, in heterogeneous neighborhoods, it is particularly important to predict and present microclimate and thermal comfort characteristics in a precise and real-time manner and to identify and determine areas with

good microclimate and thermal comfort that are suitable for outdoor activities and daily travel for the analysis of FMC walkability.

Transient and cumulative variation of thermal comfort

Since thermal comfort is the combined result of physical, physiological, and psychological responses, it exhibits spatial-temporal variations associated with a transient change of physical environment (40). Individuals can endure different levels of heat stress, due to the variation of mean radiant temperature, when walking in streets with sparse trees. During such a period, individuals may undergo a mix of conditions of heat stress aggravation, continuance, and alleviation (Figure 2), depending on the exceedance of the neutral heat stress threshold. If a thermal comfort value exceeds the neutral thermal comfort threshold, individuals will suffer from heat stress (Table 1), generating negative impacts on street walkability. Heat stress cumulates if individuals are walking in heat-positive environments continuously. In comparison, if a thermal comfort value is within or below the “no thermal stress” level, individuals will not endure heat-induced thermal stresses. The heat-stress-free level can be further divided into two sub-levels: (i) the heat stress alleviation zone, which alleviates cumulative heat stress, and (ii) the heat stress continuance zone, which neither alleviates nor strengthens the cumulative heat stress (Figure 2). Heat stress alleviation depends on the exceedance of optimal thermal comfort value.

Accordingly, individuals’ bodies endure the alternation of stress aggravation, continuance, and alleviation when they conduct activities. Heat tolerance, namely the cumulative heat stress that reaches the maximum body adaptation capacity,



is a function of aggravation, continuance, and alleviation (Equation 1).

$$F(x) = f(\text{aggravation}) + f(\text{continuance}) + f(\text{alleviation}) \quad (1)$$

Heat tolerance is also dependent on the socio-economic features of individuals (physiological response), their activity type and the alternation (behavioral feature), the clothing-related adaptive behaviors (behavioral and physical adaptation), their attention to thermal environments (psychological response), and the distance from the destination (social property). For instance, when individuals undergo severe heat stress and feel unwell during strenuous exercise, there is a high level of possibility of stopping exercising, meaning a change in heat stress aggravation to continuance or alleviation. Likewise, people may wear sun protection clothes or hold up an umbrella to shelter themselves from direct solar radiation, at which time the significant reduction of mean radiant temperature could indicate the transition from aggravation to continuance or alleviation. Limited time for commuting toward destinations (e.g., railway station, office, hospital), or visual and sound landscapes could divert their attention to thermal environments, resulting in increasing heat tolerance. Hiding in an attractive destination could potentially be an intervention of heat tolerance. Within an FMC, therefore, it is critical to consider associations between heat tolerance and social, economic, environmental, and behavioral characteristics for specific adaptation measures such as type and intensity,

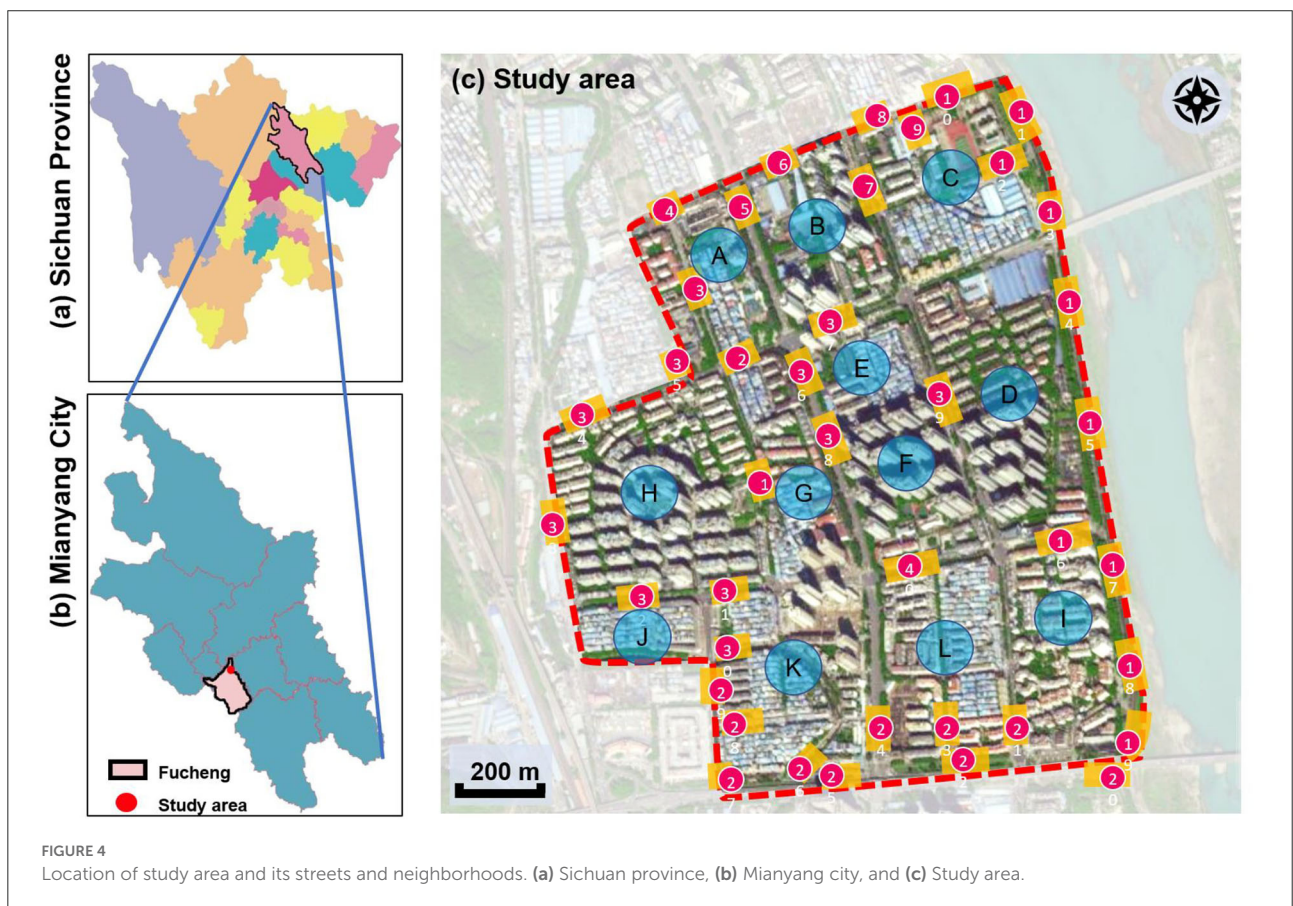
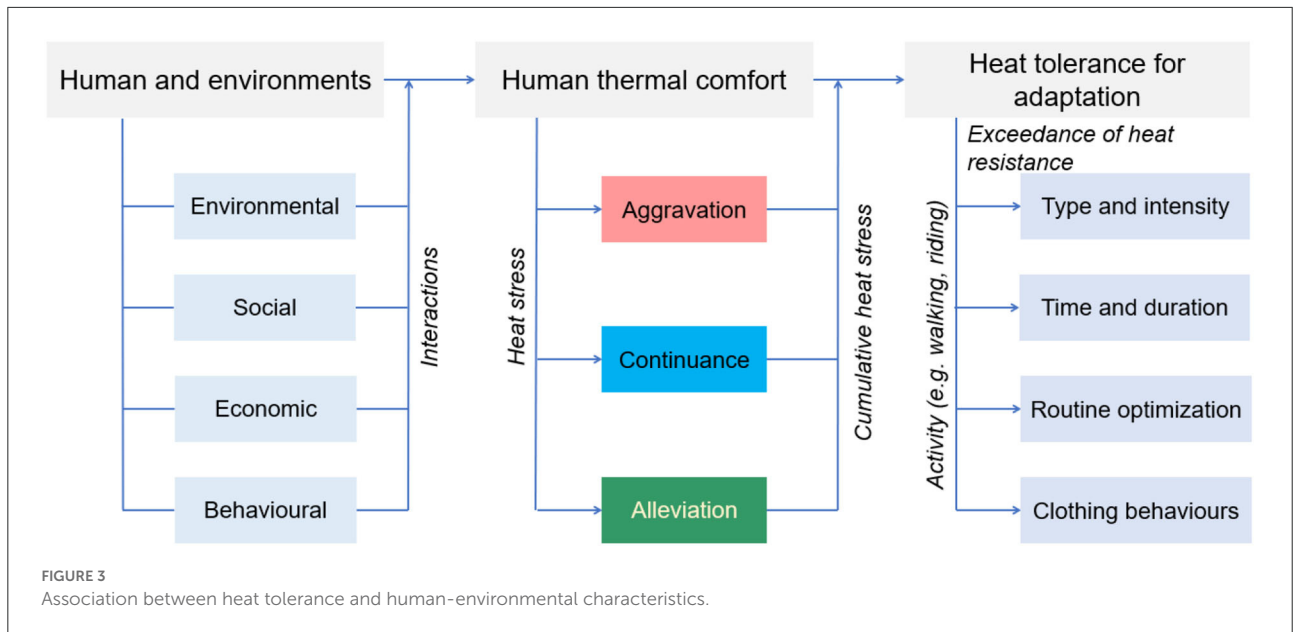
time and duration, route optimization, and clothing behaviors (Figure 3).

Case study and method

Case study area

This study was conducted in Fucheng District, Mianyang, Sichuan, China. Mianyang (30°42′-33°03′N, 103°45′-105°43′E) is the second largest prefecture-level city of Sichuan province (Figure 4), with a total area of 20,267.46 km² and a population of 4,868,243 according to the 2020 Population Census. Mianyang has an urban area of 2,755.4 km² and an urban population size of 2,232,865. It has a monsoon-influenced humid subtropical climate (Köppen Cwa) with four distinct seasons. The annual average temperature ranges between 14.7 and 17.3°C. Its summer is hot and humid, whereas July and August are the two hottest months throughout the year, with average high temperatures of 30.1 and 30.5°C, respectively.

Mianyang city is undergoing rapid urbanization, where living quality and well-being have been important concerns given the urbanization experience and lessons from various highly urbanized cities. The 15-min city concept has been integrated into urban sprawl and urban renewal to meet residents' requirements for various public service facilities relevant to daily life, leisure, and entertainment. Furthermore, the FMC underlines the proximity of fundamental public



services in the place. Such a principle requires not only the availability of public services but also the accessibility to them within FMC walkable areas. Therefore, the Gaoshui FMC in

the Fucheng district was selected to analyze the walkability. This FMC consists of 12 neighborhoods (A–L, Figure 4), within which the buildings have various ages and streets exhibit

different kinds of typology. On function type, the FMC is mainly used for residential purposes and is home to about 73,000 citizens. It also includes commercial, food, accommodation, and maintenance facilities for daily life. In particular, the flat terrain enables people to walk or ride in daily transportation functions, whereas the outdoor thermal environment is a precondition of walkability, especially in summer.

The spatial environments of the FMC exhibit a high level of heterogeneity, indicating the spatial variations of thermal environments (e.g. air temperature, wind speed, thermal comfort), and variations of walkability. Table 2 details the morphological information of 40 street scenarios presented in Figure 4c. For instance, Street 1 is well structured with mid-rise buildings, and it is almost covered by tree canopies and offers ample shade from trees and evapotranspiration cooling. Street 2 is equally well structured with dense high-rise buildings on one side and dense low-rise buildings on the other; however, there are no street trees and people can find relief only from narrow building shades. Street 11 is a riverside road with trees on both sides of the street, and the road is surrounded by a large patch of lawn. Street 24 is the main road of the city with high vehicular traffic, and trees on the street offer good and sheltered walkways protecting people from direct solar radiation. Street 26 is a pathway along with a city river and is covered by trees and an awning. The spatial variation of urban morphological characteristics is always coupled with temporal variations of thermal environments given the complex combination of time-based heat sources/sinks with morphological characteristics. Therefore, people can hardly have an intuitive assessment of street heat stress. This necessitates an accurate assessment of heat stress and associated walkability in this community.

Thermal comfort assessment indicator and dynamic attenuation model

This study adopted the UTCI as the thermal comfort assessment indicator for it presents a multi-node model of human heat transfer and temperature regulation with the consideration of clothing adaptation. Furthermore, UTCI is more sensitive to the spatial variation of thermal environments, which is capable of simulating unsteady or transient conditions. Therefore, UTCI can well respond to the frequent spatial-temporal variations of the microclimates when walking and thereby reflect the dynamic psychological responses. The UTCI is also linked with different levels of thermal sensations (Figure 5), where a heat stress level (L_{HS}) of 4 indicates an extreme heat stress level when UTCI is above 46°C.

To assess the dynamic variation of thermal comfort during walking, this study proposes a DAM of heat stress. The model defines the remaining tolerable heat discomfort (R_t) during walking with the cumulation of heat stress. In a specific duration,

the cumulation of thermal stress is defined as a function of time and heat stress level (Equation 2).

$$S_t = \sum_0^i L_{HS_i} \cdot t_i \quad (2)$$

where S_t is the cumulative heat stress with a time duration of t (Unit: min'); L_{HS_i} is the i th heat stress level, and i can be 0, 1, 2, 3, and 4; t_i is the time duration of the i th heat stress level (Unit: min).

Therefore, the remaining tolerant heat discomfort (R_t) can be expressed as:

$$R_t = H - S_t \quad (3)$$

where H is the maximum tolerant heat discomfort (Unit: min'), at which value the remaining tolerant heat discomfort R_t equals to 0, indicating that people have to stop walking to relax. Moreover, it is suggested the higher the remaining tolerant heat discomfort, the higher the walkability of the street. In an FMC, citizens are expected to be informed of the route with the highest walkability.

To determine the maximum tolerant heat discomfort H , a 15-min walkability experiment was conducted in Fucheng District, Mianyang. During the experiment, the microclimatic parameters including air temperature, wind speed, relative humidity, and mean radiant temperature were recorded for analyzing the UTCI and weighting heat stress level. A total of 128 residents attended the experiment, where they were requested to walk for 15 min at four levels of heat stress (1, 2, 3, and 4). Their perceived heat stress levels (slightly uncomfortable, uncomfortable, very uncomfortable, extremely uncomfortable) were asked and recorded at an interval of 1 min. After the experiment, the reliability analysis was carried out using SPSS 22.0. The result shows a Cronbach's α coefficient of 0.929. The Cronbach's α coefficient of each variable was above 0.8, indicating the survey results were highly reliable.

Figure 6 presents the walkable duration and respondents' discomfort level at different levels of heat stress. Respondents felt just slightly uncomfortable during their 15-min walking activity under moderate heat stress, and there were no uncomfortable, very uncomfortable, or extremely uncomfortable responses. In comparison, when respondents were under strong heat stress, they felt slightly uncomfortable in 0–8 min, while they expressed uncomfortable feelings in 9–15 min. Nevertheless, their feelings did not upscale to very uncomfortable and extremely uncomfortable levels. Under very strong heat stress, people felt slightly uncomfortable and uncomfortable in 0–5 min and 6–11 min, respectively. However, the cumulative heat stress made respondents feel very uncomfortable within 12–15 min. Under extreme heat stress, in comparison, people felt slightly uncomfortable in 0–4 min, uncomfortable in 5–7 min, very uncomfortable in 8–12 min, and extremely uncomfortable

TABLE 2 Morphological characteristics of 40 street sections.

| NO | Imagery information | Details | NO | Imagery information | Details |
|----|---|--|----|--|--|
| 1 |  | Four driveway lanes, no non-motorized lane, wide walkways, street tree canopy (~0.20 m in truck diameter), dense midrise buildings on both sides | 2 |  | Six driveway lanes, two non-motorized lanes, narrow walkways, no street tree canopy, dense low-rise or midrise buildings on both sides |
| 3 |  | Four driveway lanes, no non-motorized lane, wide walkways, street tree canopy (~0.30 m in truck diameter), dense midrise buildings on both sides | 4 |  | Four driveway lanes, no non-motorized lane, wide walkways, street tree canopy (~0.15 m in truck diameter), dense low-rise buildings on both sides |
| 5 |  | Eight driveway lanes, two non-motorized lanes, wide walkways, street tree canopy (~0.25 m in truck diameter), dense midrise buildings on both sides | 6 |  | Four driveway lanes, no non-motorized lane, wide walkways, street tree canopy (~0.25 m in truck diameter), dense low-rise buildings on both sides |
| 7 |  | Four driveway lanes, one non-motorized lane, wide walkways, street tree canopy (~0.15 m in truck diameter), dense low-rise buildings on one side and dense high-rise on the other side | 8 |  | Four driveway lanes, wide riding or walkways, street tree canopy (~0.15 m in truck diameter), dense low-rise buildings on one side and dense high-rise on the other side |
| 9 |  | Six driveway lanes, wide riding or walkways, sparse street tree canopy (~0.15 m in truck diameter), dense low-rise buildings on one side and dense high-rise buildings on the other side | 10 |  | Four driveway lanes, wide riding or walkways, sparse street tree canopy (~0.15 m in truck diameter), sparse low-rise buildings and lawns on both sides |
| 11 |  | Two driveway lanes, street tree canopy (~0.20 m in truck diameter), lawns and a narrow walkway on one side and a wide riverside walkway on the other side | 12 |  | Two driveway lanes, street tree canopy (~0.20 m in truck diameter), lawns and a wide walkway on one side, and a wide walkway and paved square on the other side |
| 13 |  | Two driveway lanes, street tree canopy (~0.20 m in truck diameter) on one side, lawns and a narrow walkway on one side and a wide riverside walkway on the other side | 14 |  | Two driveway lanes, street tree canopy (~0.20 m in truck diameter), lawns and a narrow walkway on one side and a wide riverside walkway on the other side |

(Continued)

TABLE 2 (Continued)

| NO | Imagery information | Details | NO | Imagery information | Details |
|----|---|---|----|--|--|
| 15 |  | Two driveway lanes, street tree canopy (~0.20 m in truck diameter), sunken lawns and a narrow walkway on one side and a wide riverside walkway on the other side | 16 |  | Four driveway lanes, wide walkways, street tree canopy (~0.20 m in truck diameter), dense midrise buildings on both sides |
| 17 |  | Two driveway lanes, sparse street tree canopy (~0.20 m in truck diameter), sunken lawns and a narrow walkway on one side and a wide riverside walkway on the other side | 18 |  | Two driveway lanes, street tree canopy (~0.25 m in truck diameter), sunken lawns and a narrow walkway on one side and a wide riverside walkway on the other side |
| 19 |  | Two driveway lanes, no street tree canopy, lawns and a narrow walkway on one side and an upper walkway on the other side | 20 |  | Two driveway lanes, street tree canopy (~0.20 m in truck diameter), narrow walkways on both sides |
| 21 |  | Four driveway lanes, two non-motorized lanes, wide walkways, street tree canopy (~0.15-0.20 m in truck diameter), dense midrise buildings on both sides | 22 |  | Fastway under construction, wide walkways, street tree canopy (~0.25 m in truck diameter), dense midrise buildings on one side |
| 23 |  | Two driveway lanes, wide walkways, street tree canopy (~0.20 m in truck diameter), dense midrise buildings on both sides | 24 |  | Eight driveway lanes, wide walkways, street tree canopy (~0.15-0.20 m in truck diameter), dense low buildings on both sides |
| 25 |  | Eight driveway lanes, wide walkways, street tree canopy (~0.20 m in truck diameter), dense low buildings on both sides | 26 |  | A city waterway, wide walkways, street tree canopy (~0.25 m in truck diameter), building awnings. |
| 27 |  | Four driveway lanes, wide walkways, street tree canopy (~0.20 m in truck diameter), dense low- or midrise buildings on both sides | 28 |  | Two driveway/walkway lanes, no street tree canopy (~0.20 m in truck diameter), dense midrise buildings on both sides |
| 29 |  | Four driveway lanes, wide walkways, no street tree canopy, dense midrise buildings on both sides | 30 |  | A driveway, a wide walkway, street tree canopy (~0.25 m in truck diameter), dense midrise buildings on one side and a city waterway on the other side |

(Continued)

TABLE 2 (Continued)

| NO | Imagery information | Details | NO | Imagery information | Details |
|----|---|---|----|--|--|
| 31 |  | Six driveway lanes, wide walkways, street tree canopy (~0.25 m in truck diameter) on one side, dense midrise buildings on both sides | 32 |  | Six driveway/ non-motorized lanes, wide walkways, street tree canopy (~0.20 m in truck diameter), dense midrise buildings on both sides |
| 33 |  | Six driveway/ non-motorized lanes, wide walkways, street tree canopy (~0.15–0.20 m in truck diameter) on one side, dense low-rise buildings on both sides | 34 |  | Four driveway lanes, narrow walkways, no street tree canopy, dense midrise buildings on both sides |
| 35 |  | Two driveway lanes, wide walkways, street tree canopy (~0.15 m in truck diameter), dense low-rise buildings on both sides | 36 |  | Six driveway lanes, wide walkways, street tree canopy (~0.15–0.20 m in truck diameter), dense midrise buildings on both sides |
| 37 |  | Five driveway lanes, no street tree canopy, dense high-rise buildings on both sides | 38 |  | Eight driveway lanes, two non-motorized lanes, wide walkways, street tree canopy (~0.15–0.20 m in truck diameter), dense high-rise buildings on both sides |
| 39 |  | Four driveway lanes, two non-motorized lanes, wide walkways, street tree canopy (~0.15 m in truck diameter), dense midrise buildings on both sides | 40 |  | Four driveway/non-motorized lanes, wide walkways, street tree canopy (~0.15 m in truck diameter), dense low-rise buildings on both sides |

| Thermal stress | Extreme cold stress | Very strong cold stress | Strong cold stress | Moderate cold stress | Slight cold stress | No thermal stress | Moderate heat stress | Strong heat stress | Very strong heat stress | Extreme heat stress |
|--|---------------------|-------------------------|--------------------|----------------------|--------------------|-------------------|----------------------|--------------------|-------------------------|---------------------|
| Heat stress level | -5 | -4 | -3 | -2 | -1 | 0 | 1 | 2 | 3 | 4 |
| Universal Thermal Climate Index (UTCI, °C) | <-40 | -40 – -27 | -27 – -13 | -13 – -0 | 0 – 9 | 9 – 26 | 26 – 32 | 32 – 38 | 38 – 46 | >46 |

FIGURE 5 Association between heat stress levels and UTCI.

| Heat stress level | | Moderate heat stress | Strong heat stress | Very strong heat stress | Extreme heat stress |
|---|-------------------------|----------------------|--------------------|-------------------------|---------------------|
| | | Level 1 | Level 2 | Level 3 | Level 4 |
| Walkable duration under different levels of heat stress (min) | Slightly uncomfortable | 0-15 | 0-8 | 0-5 | 0-4 |
| | Uncomfortable | | 9-15 | 6-11 | 5-7 |
| | Very uncomfortable | | | 12-15 | 8-12 |
| | Extremely uncomfortable | | | | 13-15 |

FIGURE 6
Heat stress level and its impact on walkable duration.

in 13–15 min. Therefore, a walkable duration of 13–15 min under Level 4 heat stress suggested a maximum tolerant heat discomfort H ranging between 52–60 min. In this study, an aspirational value of 60 min was considered. It should be noted that the walkable duration and associated maximum tolerant heat discomfort had already included physical, psychological, and physiological responses of respondents, rather than only considering physical environments.

Accordingly, the remaining tolerant heat discomfort (R_t) is:

$$R_t = 60 - S_t \quad (4)$$

Numerical simulations of 15-min city thermal environments

To estimate spatial-temporal variations of thermal environments and associated heat stress, the ENVI-met model (Science version) was adopted. The ENVI-met model is currently the most holistic, three-dimensional microclimate model to present the high-resolution interactions among surfaces, plants, and the atmosphere. It has been widely adopted to calculate block- and neighborhood-scale microclimate and heat stress for climate-sensitive urban planning. The urban morphology, street network, tree planting and species, surface structure, and surface texture were obtained through satellite images, local urban planning council, and field observation. Given the large study area, we set $200 \times 240 \times 40$ grids in horizontal, perpendicular, and vertical directions, with a grid resolution of 8 meters.

Weather condition is also important to simulate the ENVI-met model. The two hottest months of Mianyang are July and August. According to the data from China Meteorological Administration, an average temperature of 28°C was the most prominent in 2020 and mainly occurred in August. Therefore,

typical weather conditions (wind direction, wind speed, air temperature, and relative humidity) were adopted for the simulation (Table 3). In the daytime, the temperatures were generally high and the walkable duration generally occurred between 8:00 and 19:00 h. In particular, the peak walking periods were 8:00–9:00 h and 17:00–18:00 h, when people go to and return from work. Compared with 8:00–9:00 h, the temperature at 17:00–18:00 h was much higher and heat stress was much worse, so the period returning from work was particularly analyzed.

Note that the above-mentioned simulation settings have been adopted to demonstrate the applicability of the DAM in walkable route planning. Comprehensive planning for a walkable route should be presented hour-by-hour, and the resolution should be higher to capture spatial heterogeneity of street sections, building heights, and tree heights. Moreover, to ensure people are better protected, an hour-to-hour local weather boundary condition, rather than the data from national weather stations which always fail to accurately present local climates, is needed to precisely capture the real-time maximum temperature and heat stress.

Result analysis and discussion

Verification of spatial heterogeneity of thermal comfort

Figure 7 presents the simulated thermal comfort (UTCI) of the FMC between 17:00 and 18:00 h. The UTCI ranged between 31.26 and 40.86°C , primarily showing strong heat stress and very strong heat stress that could be categorized as Level-2 and Level-3 heat stress (Figure 5). The thermal comfort distribution was highly heterogeneous. Overall, the thermal environments within each neighborhood were much better than on the streets. This was mainly linked to building shades, tree canopies, and grassland within the community. Nevertheless,

TABLE 3 Weather data adopted to simulate the ENVI-met model.

| Data category | Detail | Data category | Detail |
|---------------------|----------------------------------|---------------------------|----------------|
| Geographic location | 30°42′-33°03′N, 103°45′-105°43′E | Minimum air temperature | 24.6°C (07:00) |
| Simulation time | 0:00-19:00 | Maximum air temperature | 32°C (15:00) |
| wind direction | 245° | Minimum relative humidity | 66% (17:00) |
| wind speed | 1.4 m/s | Maximum relative humidity | 94% (09:00) |

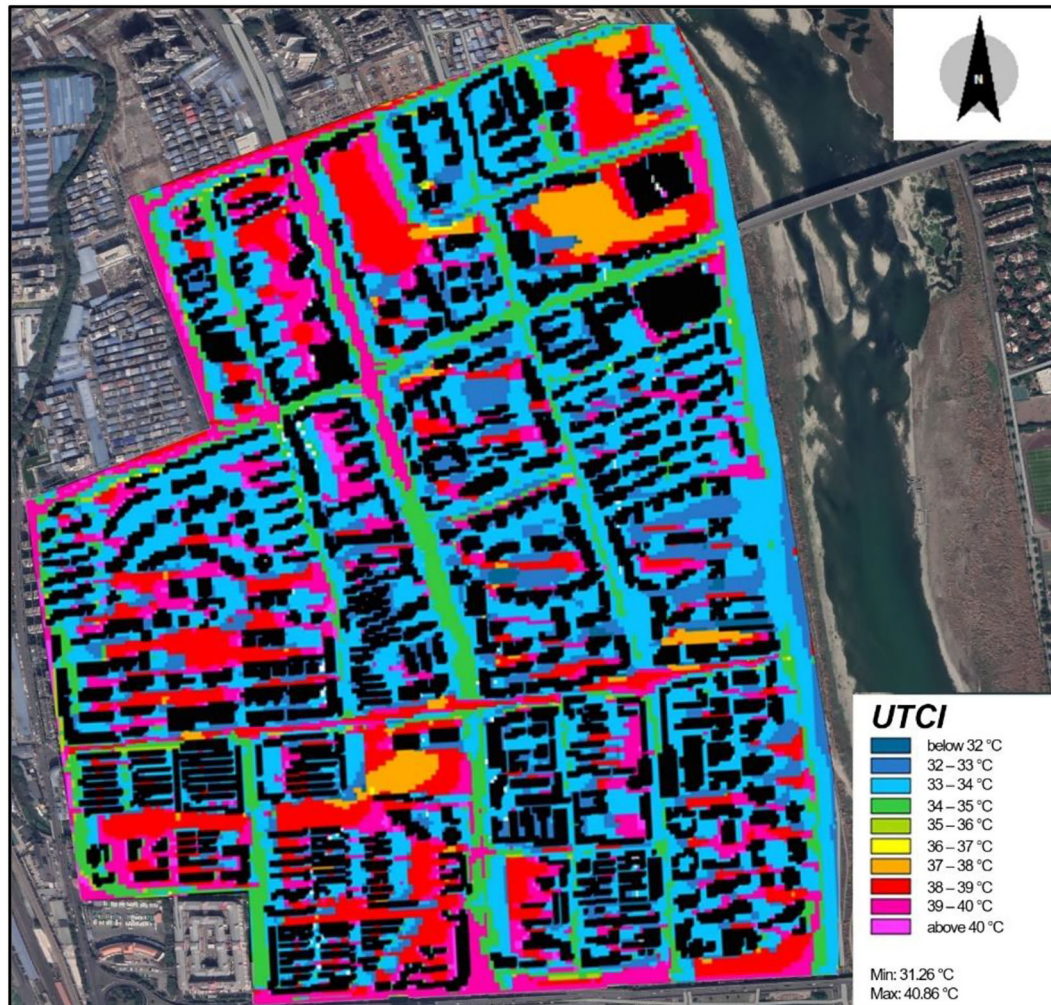


FIGURE 7
Distribution of simulated UTCI of the study area.

the neighborhoods were dense and enclosed, and in areas that were paved with cement and under direct solar exposure, the thermal environments were much worse. The riverside streets (Street 11-19) presented a good thermal environment with the UTCI ranging between 32 and 34°C. In comparison, north-south streets at 33-34°C exhibited a lower UTCI level

than east-west streets at 36-40°C. The results are also dependent on the height of the buildings on the street. For instance, the middle section of streets 5 and 36 with low and mid-rise buildings had a higher UTCI level of 39-40°C than Street 38 with mid- and high-rise buildings at 33-35°C. Similarly, in streets 5 and 36, their central section was warmer than the

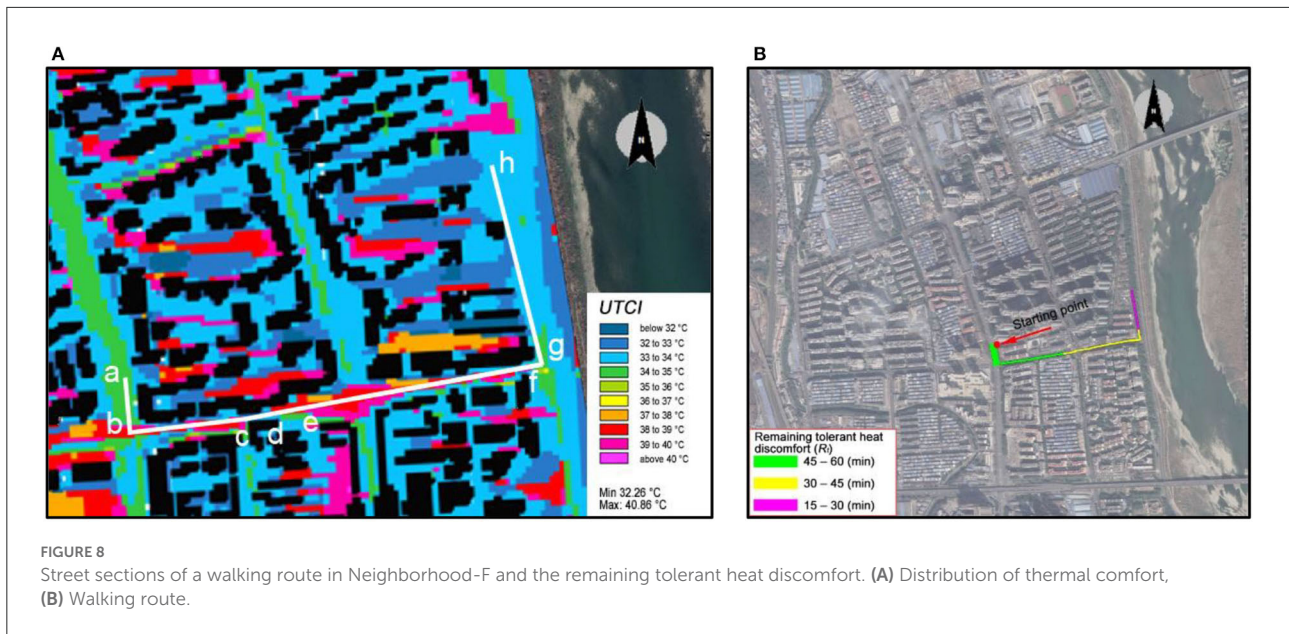


FIGURE 8 Street sections of a walking route in Neighborhood-F and the remaining tolerant heat discomfort. (A) Distribution of thermal comfort, (B) Walking route.

TABLE 4 Dynamic variation of the remaining tolerant heat discomfort of a walking route of Neighborhood-F.

| Street | UTCI (°C) | LHS | Street distance (m) | Walking duration (min) | R _t (min) |
|--------|-----------|-----|---------------------|------------------------|----------------------|
| ab | 34–36 | 2 | 71.1 | 1.2 | 57.6 |
| bc | 38–40 | 3 | 171.7 | 2.9 | 48.9 |
| cd | 33–34 | 2 | 44.8 | 0.8 | 47.3 |
| de | 38–40 | 3 | 51.0 | 0.9 | 44.6 |
| ef | 37–40 | 3 | 292.0 | 4.9 | 29.9 |
| fg | 33–36 | 2 | 12.0 | 0.2 | 29.5 |
| gh | 32–36 | 2 | 257.3 | 4.3 | 20.9 |

sides due to the shade from trees and buildings. The results also indicate an open and wide street adjacent to the river could have a better thermal environment, for instance, Street 37 at 34–35°C.

Assessment of street walkability

According to the municipal roads and land boundaries within the study area, 12 neighborhoods were identified (Figure 4). Setting the entrance of these neighborhoods as the starting points for daily walking, the walking routes were analyzed taking into consideration heat stress. The maximum walkable distance was set as 900 m based on a walking speed of 1 m/s. Figure 8A exhibits a possible walking route (a-h) of Neighborhood-F, (Figure 5), and the DAM (Equations 2,4), the remaining tolerant heat discomfort was calculated, as shown in Table 4.

The results indicate that section ab had a UTCI range of 34–36°C, namely a heat stress level of 2. Its street distance of 71.1 m, corresponding to a walking duration of 1.2 min, led to

cumulative thermal stress of 2.4 min, and thereby a remaining tolerant heat discomfort of 57.6 min, based on the maximum tolerant heat discomfort of 60 min. Following this, from point-a to point-h, the remaining tolerant heat discomfort for 900 m was 20.9 min. As shown in Figure 8B, in particular, the section ae had an R_t of 45–60 min, section e, g, 30–45 min, and section gh had 15–30 min.

Likewise, 15-min walkable routes were identified, as shown in Figure 9. It was observed that the 15-min walkable routes of neighborhoods A, B, C, D, and E were mainly in green and yellow color, representing a remaining tolerant heat discomfort above 30 min. In comparison, other neighborhoods presented green, yellow, and purple colors, indicating a remaining tolerant heat discomfort above 15 min. Such a comparison further indicates that neighborhoods F-L were more vulnerable in the 15-min walkability. While such results could directly help identify the travel paths for citizens to avoid strong heat stress, the results also suggest that there is a need to adopt urban heat mitigation and adaptation techniques and strategies to improve heat resilience. Different from existing studies on

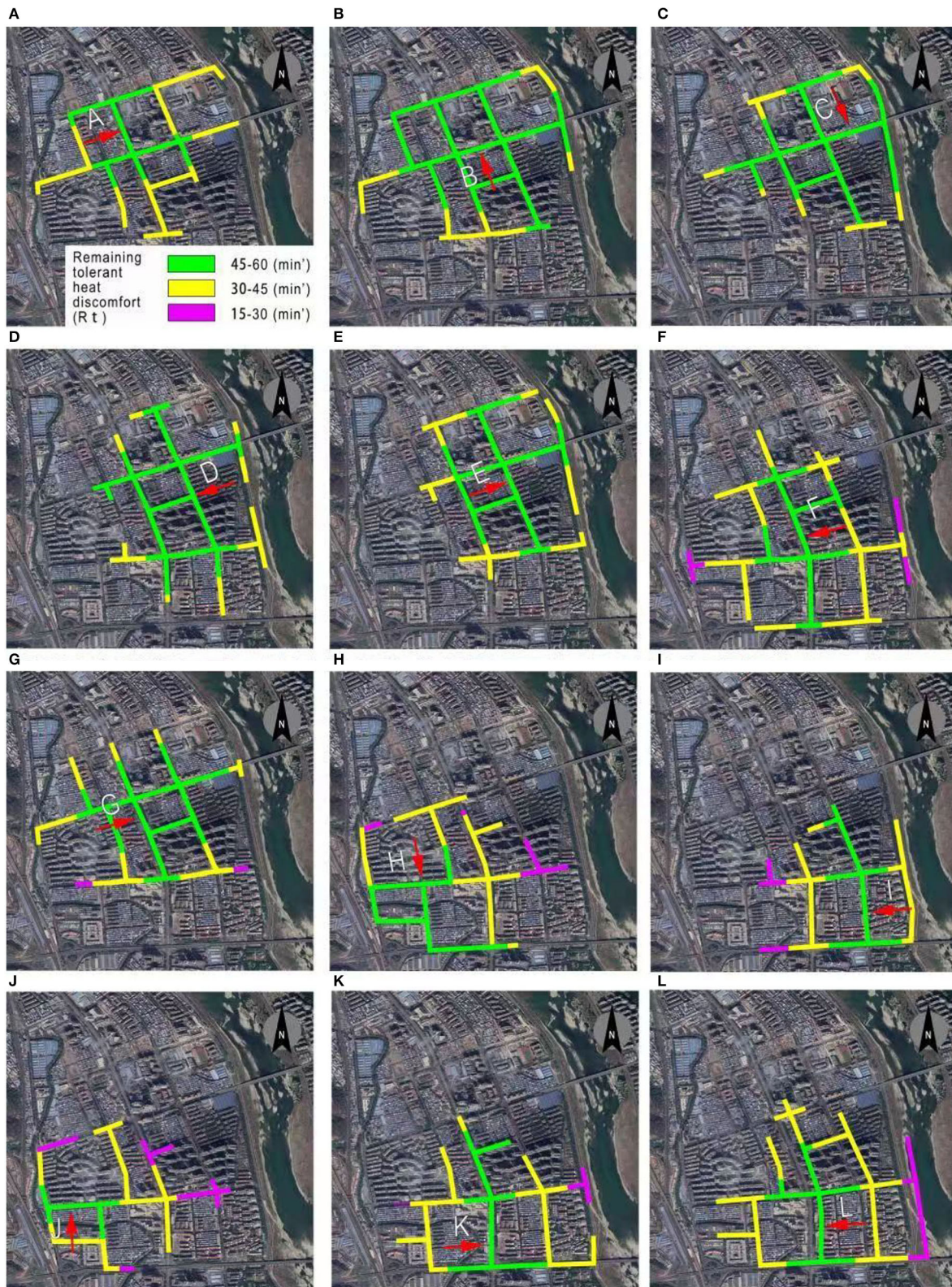


FIGURE 9 Identification of remaining tolerant heat discomfort of all possible walkable routes of 12 neighborhoods. (A) Neighborhood-A, (B) Neighborhood-B, (C) Neighborhood-C, (D) Neighborhood-D, (E) Neighborhood-E, (F) Neighborhood-F, (G) Neighborhood-G, (H) Neighborhood-H, (I) Neighborhood-I, (J) Neighborhood-J, (K) Neighborhood-K, (L) Neighborhood-L.

dealing with heat stress by adding location-based interventions, the current walkability-based study provides new insights into planning-based adaptation. For instance, for the walkable routes in Neighborhood-F (Table 4), interventions added to improve thermal environments in a-h sections can potentially improve the path walkability by reducing the heat stress of any section.

Assessment of the FMC walkability and implications

To support the FMC planning and design, this study further assessed the overall walkability of the study area. Based on street walkability (Figure 9), a population-based weighting algorithm (Equation 5) was adopted to adjust the heat stress of each street.

$$k_i = \frac{P_i}{\sum_1^n P_i} \quad (5)$$

Where, k_i is the weight of each neighborhood in the 15-min city; P_i is the population number of each neighborhood; and n is the total number of neighborhoods, set as 12 in this study.

The weight k_i of each neighborhood is presented in Table 5.

The overall street walkability of the FMC, after taking into consideration heat stress, is generated in Figure 10A. Overall, the central part exhibited the highest remaining tolerant heat discomfort, while the outmost areas had the lowest remaining tolerant heat discomfort. To improve walkability, there is a need to focus on the improvement of thermal environments. In general, it is better to improve the walkability of the central parts (with the highest weight) to extend the overall walkability. However, in this study, the central areas generally had a low UTCI (Figure 7) and weak heat stress so adding interventions in the central parts did not exhibit high potential. Instead, adding cooling interventions in the yellow section could help weaken heat stress and extend street walkability the most. The improvement of the thermal environments of the purple section is also recommended.

The overall walkability also generates implications on the configuration of public service which is a typical adaptation measure to reduce citizens' heat stress by foot. The public service was divided into three types, according to the visiting frequency: frequently-used, often-used, occasionally-used, and indirectly-used (Table 5). In general, the indirectly-used public service is the one people do not visit directly or seldom visit, so it was not considered in this study. Figure 10B presents possible locations of frequently-used, often-used, and occasionally-used public services. The frequently-used public service was configured at the street sections with the highest remaining tolerant heat discomfort, and the occasionally-used public service was set at the street sections with the lowest remaining tolerant heat discomfort. The often-used one was set in the green-yellow transition street section or a green section. Our empirical work also found that various existing public services

which are frequently used and often used were configured in yellow- and purple-colored street sections, making many citizens rely on private cars rather than walking. Therefore, urban heat mitigation strategies should be added to improve the thermal environment and street walkability. Simultaneously, public services should be gradually relocated to improve the accessibility of public services within walkable areas.

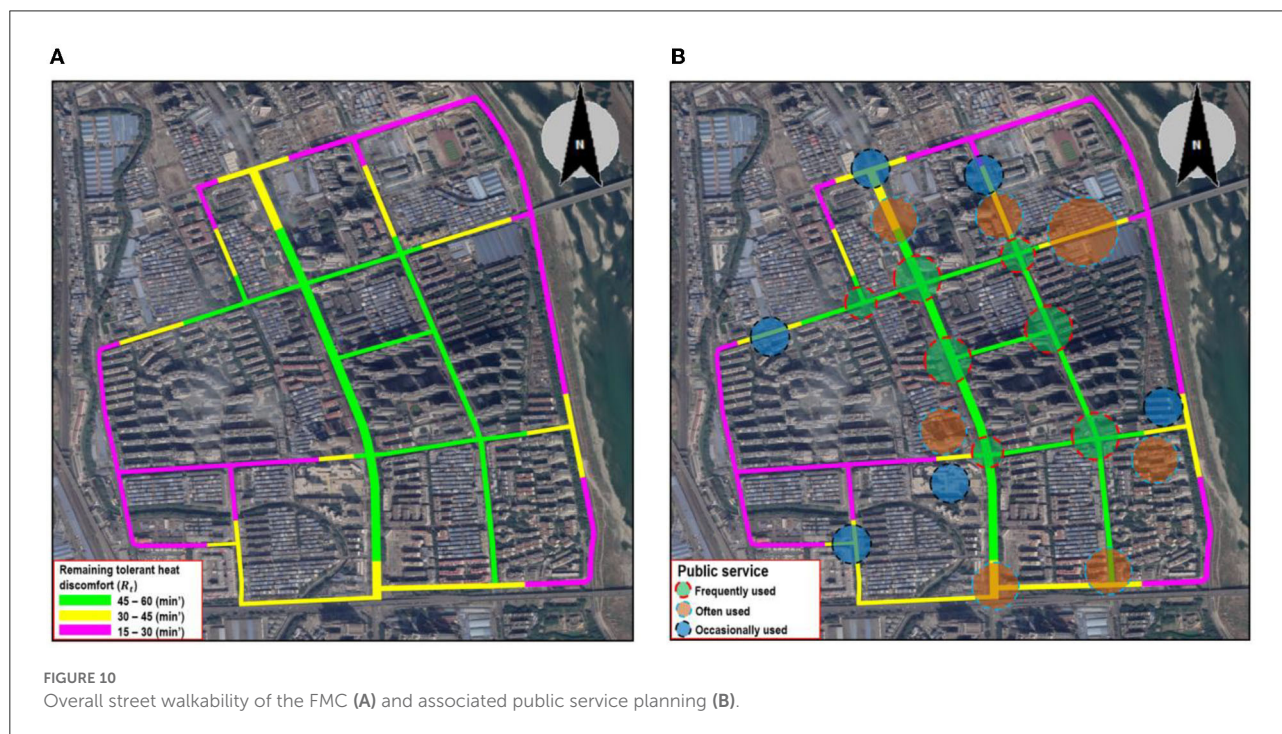
Conclusion

The FMC concept has been implemented in various countries to build high-quality cities. Whilst the goals of inclusiveness, safety, and health have been widely accepted, the achievement of such goals is compromised since inclusiveness, safety, and health are interlinked with various factors. This study considered the issue of urban heat which is increasingly severe along with climate change and urbanization. This is a pioneering study on integrating heat-related impacts within the FMC framework by investigating walkability and developing a dynamic attenuation model (DAM) of heat stress. The model was applied to an FMC in Fucheng District, Mianyang, China. Some imperative results that were suitable for the case study have been obtained, and the results could generate implications for the (re)configuration of public services in urban planning and design. Overall, the findings could provide a practical reference for urban heat mitigation and adaptation. This paper has also meaningfully added new knowledge on heat-related FMC planning and design.

Whilst this study is the first one on the integration of heat-related walkability into the FMC concept, there are some limitations that should be considered. First, the remaining tolerant heat discomfort was developed based on the empirical study among 128 interviewees; the sample size might not be large enough to completely represent everyone's heat tolerance, and the empirical study had not integrated socioeconomic characteristics and public services that might intervene in people's heat responses for comprehensively assessing walkability. In particular, for vulnerable groups including children, older adults, and pregnant women, there should be an accurate heat stress threshold. Second, this study set four levels of heat stress for determining the remaining tolerant heat discomfort, while the constant heat stress could not present the variability of the thermal comfort and heat stress. As a result, the heat aggravation, continuance, and alleviation had not been well considered. Third, the model adopted the UTCI to assess the heat stress, while the capacity of other outdoor thermal comfort indicators such as PET, and WBGT had not been used in this study. Fourth, the study adopted an FMC in Fucheng as the case study. Whilst the results can provide strong implications for FMC planning and design, the applicability of the results for other cities might be uncertain since the clothing behaviors and heat-resistant capacity could vary with regions. Fifth, heat-induced impacts on thermal comfort happen throughout the

TABLE 5 Weight of each neighborhood for adjusting street walkability of the study area.

| Block | A | B | C | D | E | F | G | H | I | J | K | L |
|----------------|------|------|------|------|------|------|------|------|------|------|------|------|
| Population (k) | 3.0 | 2.7 | 2.2 | 12.7 | 2.7 | 6.1 | 3.4 | 8.2 | 2.8 | 6.2 | 9.8 | 13.0 |
| Weight k_i | 0.04 | 0.04 | 0.03 | 0.17 | 0.04 | 0.08 | 0.05 | 0.11 | 0.04 | 0.09 | 0.13 | 0.18 |



day, especially in the daytime, while this study only considered the period between 17:00 and 18:00 h for walkability assessment and walkable route determination. Planning suggestions on public services were also given based on this time period, which could lead to biases if an urban design scheme was implemented based on the results presented in this paper. More efforts should be conducted to improve DAM accuracy, especially in social-economic, spatial, and temporal aspects, for broad applicability.

Data availability statement

The raw data supporting the conclusions of this article will be made available by the authors, without undue reservation.

Author contributions

YW: conceptualization, formal analysis, funding acquisition, investigation, methodology, software, validation, visualization, roles, and writing—original draft. B-JH: conceptualization, funding acquisition, project administration, methodology, resources, visualization, and writing—review and editing. CK and XC: investigation, methodology, and writing—review

and editing. LY: investigation, methodology, and writing—review and editing. MY: investigation, and methodology. XL: conceptualization, formal analysis, and writing—review and editing. TZ: supervision, project administration, resources, and writing—review and editing. All authors contributed to the article and approved the submitted version.

Funding

Project no. 2021CDJQY-004 was supported by the Fundamental Research Funds for the Central Universities; State Key Laboratory of Subtropical Building Science, South China University of Technology (Grant Nos. 2022ZA01 and 2021ZB16). Graduate Scientific Research and Innovation Foundation of Chongqing, China (CYB22058). Special thanks go to the National Natural Science Foundation of China (Grant No. 52108011); Guangzhou Philosophy and Social Science Planning 2022 Annual Project (Grant No. 2022GZQN14); China Postdoctoral Science Foundation (Grant No. 2021M701249); Department of Education of Guangdong Province (Grant No. 2021KTSCX004); Science and Technology Program of Guangzhou, China (Grant No. 202102020302);

and Department of Housing and Urban-Rural Development of Guangdong Province (Grant No. 2021-K2-305243).

Acknowledgments

Many thanks go to the support of attendees for the walkable duration assessment.

Conflict of interest

XL was employed by Architectural Design and Research Institute Co., Ltd.

References

- United Nations. *World Population Prospects: The 2017 Revision, Key Findings and Advance Tables*. Department of Economics Social Affairs. New York: United Nations (2017).
- Hong X-C, Wang G-Y, Liu J, Song L, Wu ETY. Modeling the impact of soundscape drivers on perceived birdsongs in urban forests. *J Clean Prod.* (2021) 292:125315. doi: 10.1016/j.jclepro.2020.125315
- Marazziti D, Cianconi P, Mucci F, Foresi L, Chiarantini I, Della Vecchia A. Climate change, environment pollution, COVID-19 pandemic and mental health. *Sci. Total Environ.* (2021) 773:145182. doi: 10.1016/j.scitotenv.2021.145182
- Liu Y, Gao H, Cai J, Lu Y, Fan Z. Urbanization path, housing price and land finance: International experience and China's facts. *Land Use Policy.* (2022) 113:105866. doi: 10.1016/j.landusepol.2021.105866
- Hughes L, Hanna E, Fenwick J. The silent killer: climate change and the health impacts of extreme heat. Climate Council of Australia Limited (2016).
- Iping A, Kidston-Lattari J, Simpson-Young A, Duncan E, McManus P. (Re) presenting urban heat islands in Australian cities: a study of media reporting and implications for urban heat and climate change debates. *Urban Climate.* (2019) 27:420–9. doi: 10.1016/j.uclim.2018.12.014
- Rizwan AM, Dennis LYC, Liu C. A review on the generation, determination and mitigation of Urban Heat Island. *J Environ Sci.* (2008) 20:120–8. doi: 10.1016/S1001-0742(08)60019-4
- Arnfield AJ. Two decades of urban climate research: a review of turbulence, exchanges of energy and water, and the urban heat island. *Int J Climatol.* (2003) 23:1–26. doi: 10.1002/joc.859
- Oke TR, Mills G, Christen A, Voogt JA. *Urban Climates*. Cambridge: Cambridge University Press (2017).
- Santamouris M, Kolokotsa D. On the impact of urban overheating and extreme climatic conditions on housing, energy, comfort and environmental quality of vulnerable population in Europe. *Energy Buildings.* (2015) 98:125–33. doi: 10.1016/j.enbuild.2014.08.050
- City of Sydney. *Adapting for Climate Change: A Long Term Strategy for the City of Sydney*. City of Sydney, NSW (2015).
- De Bono A, Peduzzi P, Kluser S, Giuliani G. Impacts of summer 2003 heat wave in Europe. *Environment Alert Bulletin.* (2004) 2:4. Available online at: https://www.unisdr.org/files/1145_ewheatwave.en.pdf
- Anderson GB, Bell Michelle L. Heat waves in the United States: mortality risk during heat waves and effect modification by heat wave characteristics in 43 US communities. *Environ Health Perspect.* (2011) 119:210–8. doi: 10.1289/ehp.1002313
- Robine JM, Cheung SLK, Le Roy S, Van Oyen H, Griffiths C, Michel JP, et al. Death toll exceeded 70,000 in Europe during the summer of 2003. *C R Biol.* (2008) 331:171–8. doi: 10.1016/j.crvi.2007.12.001
- EEA. Extreme temperatures and health. European Environment Agency (2021). Available online at: https://www.eea.europa.eu/data-and-maps/indicators/heat-and-health-2/assessment/#_edn3 (accessed October 20, 2021).
- Public Health England. Heatwave mortality monitoring report: 2020 (2020). Available online at: <https://www.gov.uk/government/publications/phe-heatwave-mortality-monitoring/heatwave-mortality-monitoring-report-2020> (accessed November 19, 2020).
- McLaren D. Guest post: The problem with net-zero emissions targets. Carbon Brief, (2019). Available online at: <https://www.carbonbrief.org/guest-post-the-problem-with-net-zero-emissions-targets> (accessed September 19, 2019).
- Roth M. *Urban Heat Islands, in Handbook of Environmental Fluid Dynamics*. Boca Raton, FL: CRC Press (2012), p. 162–81.
- He B-J, Wang J, Liu H, Ulpiani G. Localized synergies between heat waves and urban heat islands: Implications on human thermal comfort and urban heat management. *Environ Res.* (2021) 193:110584. doi: 10.1016/j.envres.2020.110584
- He B-J, Zhao D, Xiong K, Qi J, Ulpiani G, Pignatta G, et al. framework for addressing urban heat challenges and associated adaptive behavior by the public and the issue of willingness to pay for heat resilient infrastructure in Chongqing, China. *Sustainable Cities Soc.* (2021) 75:103361. doi: 10.1016/j.scs.2021.103361
- Zhang G, He B-J, Dewancker BJ. The maintenance of prefabricated green roofs for preserving cooling performance: A field measurement in the subtropical city of Hangzhou, China. *Sustainable Cities Soc.* (2020) 61:102314. doi: 10.1016/j.scs.2020.102314
- Ampatzidis P, Kershaw T. A review of the impact of blue space on the urban microclimate. *Sci Total Environ.* (2020) 730:139068. doi: 10.1016/j.scitotenv.2020.139068
- Wang C, Wang Z-H, Kaloush KE, Shacat J. Cool pavements for urban heat island mitigation: a synthetic review. *Renewable Sustainable Energy Rev.* (2021) 146:111171. doi: 10.1016/j.rser.2021.111171
- Rawat M, Singh RN. A study on the comparative review of cool roof thermal performance in various regions. *Energy Built Environ.* (2021) 3:327–47. doi: 10.1016/j.enbenv.2021.03.001
- He B-J, Ding L, Prasad D. Wind-sensitive urban planning and design: Precinct ventilation performance and its potential for local warming mitigation in an open midrise gridiron precinct. *J Build Eng.* (2020) 29:101145. doi: 10.1016/j.jobbe.2019.101145
- He B-J, Ding L, Prasad D. Relationships among local-scale urban morphology, urban ventilation, urban heat island and outdoor thermal comfort under sea breeze influence. *Sust Cities Soc.* (2020) 60:102289. doi: 10.1016/j.scs.2020.102289
- Elgheznavy D, Eltarabily S. The impact of sun sail-shading strategy on the thermal comfort in school courtyards. *Build Environ.* (2021) 202:108046. doi: 10.1016/j.buildenv.2021.108046
- Tamaskani Esfehankalateh A, Ngarambe J, Yun GY. Influence of tree canopy coverage and leaf area density on urban heat island mitigation. *Sustainability.* (2021) 13:7496. doi: 10.3390/su13137496
- He B-J, Zhu J, Zhao D-X, Gou Z-H, Qi J-D, Wang J. Co-benefits approach: Opportunities for implementing sponge city and urban heat island mitigation. *Land Use Policy.* (2019) 86:147–57. doi: 10.1016/j.landusepol.2019.05.003

The remaining authors declare that the research was conducted in the absence of any commercial or financial relationships that could be construed as a potential conflict of interest.

Publisher's note

All claims expressed in this article are solely those of the authors and do not necessarily represent those of their affiliated organizations, or those of the publisher, the editors and the reviewers. Any product that may be evaluated in this article, or claim that may be made by its manufacturer, is not guaranteed or endorsed by the publisher.

30. Drinkwater BL, Horvath SM. Heat tolerance and aging. *Med Sci Sports*. (1979) 11:49–55.
31. He B-J, Zhao D, Dong X, Xiong K, Feng C, Qi Q, et al. Perception, physiological and psychological impacts, adaptive awareness and knowledge, and climate justice under urban heat: A study in extremely hot-humid Chongqing, China. *Sustainable Cities Soc.* (2022) 79:103685. doi: 10.1016/j.scs.2022.103685
32. Dunne JP, Stouffer RJ, John JG. Reductions in labour capacity from heat stress under climate warming. *Nat Clim Chang.* (2013) 3:563–6. doi: 10.1038/nclimate1827
33. Raya AB, Hasibuan HS, Sodri A. Thermal comfort-based spatial planning model in jakarta transit-oriented development (TOD). *Atmosphere.* (2022) 13:565. doi: 10.3390/atmos13040565
34. He B-J, Wang J, Zhu J, Qi J. Beating the urban heat: Situation, background, impacts and the way forward in China. *Renewable Sust Energ Rev.* (2022) 161:112350. doi: 10.1016/j.rser.2022.112350
35. Kotharkar R, Ghosh A. Progress in extreme heat management and warning systems: A systematic review of heat-health action plans (1995–2020). *Sust Cities Soc.* (2022) 76:103487. doi: 10.1016/j.scs.2021.103487
36. Pozoukidou G, Chatziyiannaki Z. 15-minute city: decomposing the new urban planning Eutopia. *Sustainability.* (2021) 13:928. doi: 10.3390/su13020928
37. Chen X, He B-J. Development of a framework for urban heat adaptation in 15-minute city. In *SBEfin 2022 Conference - Emerging Concepts for Sustainable Built Environment*, Helsinki, Finland (2022).
38. Chen S, Wang T, Bao Z, Lou V. A path analysis of the effect of neighborhood built environment on public health of older adults: a Hong Kong study. *Front Pub Health.* (2022) 10:861836. doi: 10.3389/fpubh.2022.861836
39. Chen S, Bao Z, Lou V. Assessing the impact of the built environment on healthy aging: a gender-oriented Hong Kong study. *Environ Impact Assess Rev.* (2022) 95:106812. doi: 10.1016/j.eiar.2022.106812
40. Cheng Y, Niu J, Gao N. Thermal comfort models: A review and numerical investigation. *Build Environ.* (2012) 47:13–22. doi: 10.1016/j.buildenv.2011.05.011
41. Kumar P, Sharma A. Study on importance, procedure, and scope of outdoor thermal comfort –A review. *Sust Cities Soc.* (2020) 61:102297. doi: 10.1016/j.scs.2020.102297
42. Chen L, Ng E. Outdoor thermal comfort and outdoor activities: A review of research in the past decade. *Cities.* (2012) 29:118–25. doi: 10.1016/j.cities.2011.08.006
43. Inavonna I, Hardiman G, Purnomo AB. Outdoor thermal comfort and behaviour in urban area. *IOP Conf Series Earth Environ Sci.* (2018) 106:012061. doi: 10.1088/1755-1315/106/1/012061
44. Ergonomics of the Thermal Environment. *Analytical Determination and Interpretation of Thermal Comfort using Calculation of the PMV and PPD Indices and Thermal Comfort Criteria*. Geneva: International Organisation for Standardisation (ISO) (200), p. 1–36.
45. Ioannou LG, Mantzios K, Tsoutsoubi L, Notley SR, Dinas PC, Brearley M, et al. Indicators to assess physiological heat strain – Part 1: systematic review. *Temperature.* (2022) 31:1–36. doi: 10.1080/23328940.2022.2037376
46. Grundstein A, Williams C, Phan M, Cooper E. Regional heat safety thresholds for athletics in the contiguous United States. *Appl Geograp.* (2015) 56:55–60. doi: 10.1016/j.apgeog.2014.10.014
47. Matzarakis A, Muthers S, Koch E. Human biometeorological evaluation of heat-related mortality in Vienna. *Theor App Climatol.* (2011) 105:1–10. doi: 10.1007/s00704-010-0372-x
48. Lin T-P, Matzarakis A. Tourism climate and thermal comfort in Sun Moon Lake, Taiwan. *Int J Biometeorol.* (2008) 52:281–90. doi: 10.1007/s00484-007-0122-7
49. Błazejczyk K, Jendritzky G, Bröde P, Fiala D, Havenith G, Epstein Y, et al. Kampmann BJGP. An introduction to the universal thermal climate index (UTCI). *Geo. Pol.* (2013) 86:5–10. doi: 10.7163/GPol.2013.1
50. Kuchcik M. Mortality and thermal environment (UTCI) in Poland—long-term, multi-city study. *Int J Biometeorol.* (2021) 65:1529–41. doi: 10.1007/s00484-020-01995-w
51. Morakinyo TE, Dahanayake KWDC, Adegun OB, Balogun AA. Modelling the effect of tree-shading on summer indoor and outdoor thermal condition of two similar buildings in a Nigerian university. *Energy Buildings.* (2016) 130:721–32. doi: 10.1016/j.enbuild.2016.08.087
52. Imam Syafii N, Ichinose M, Kumakura E, Jusuf SK, Chigusa K, Wong NH. Thermal environment assessment around bodies of water in urban canyons: A scale model study. *Sust Cities Soc.* (2017) 34:79–89. doi: 10.1016/j.scs.2017.06.012
53. Johansson E. Influence of urban geometry on outdoor thermal comfort in a hot dry climate: a study in Fez, Morocco. *Build Environ.* (2006) 41:1326–38. doi: 10.1016/j.buildenv.2005.05.022
54. Giannopoulou K, Santamouris M, Livada I, Georgakis C, Caouris Y. The impact of canyon geometry on intra urban and urban: suburban night temperature differences under warm weather conditions. *Pure App Geophys.* (2010) 167:1433–49. doi: 10.1007/s00024-010-0099-8
55. Santamouris M, Gaitani N, Spanou A, Saliari M, Giannopoulou K, Vasilakopoulou K, et al. Using cool paving materials to improve microclimate of urban areas – Design realization and results of the flisvos project. *Build Environ.* (2012) 53:128–36. doi: 10.1016/j.buildenv.2012.01.022
56. Chang C-R, Li M-H, Chang S-D. A preliminary study on the local cool-island intensity of Taipei city parks. *Landsc Urban Plan.* (2007) 80:386–95. doi: 10.1016/j.landurbplan.2006.09.005
57. Tran DX, Pla F, Latorre-Carmona P, Myint SW, Caetano M, Kieu HV. Characterizing the relationship between land use land cover change and land surface temperature. *ISPRS J Photogram Remote Sensing.* (2017) 124:119–32. doi: 10.1016/j.isprsjprs.2017.01.001
58. Sanaieian H, Tenpierik M, van den Linden K, Seraj FM, Shemrani SMM. Review of the impact of urban block form on thermal performance, solar access and ventilation. *Renewable Sust Energ Rev.* (2014) 38:551–60. doi: 10.1016/j.rser.2014.06.007
59. Tong S, Wong NH, Jusuf SK, Tan CL, Wong HF, Ignatius M, et al. Study on correlation between air temperature and urban morphology parameters in built environment in northern China. *Build Environ.* (2018) 127:239–49. doi: 10.1016/j.buildenv.2017.11.013
60. Emmanuel R, Johansson E. Influence of urban morphology and sea breeze on hot humid microclimate: the case of Colombo, Sri Lanka. *Climate Res.* (2006) 30:189–200. doi: 10.3354/cr030189
61. Ali-Toudert F, Mayer H. Numerical study on the effects of aspect ratio and orientation of an urban street canyon on outdoor thermal comfort in hot and dry climate. *Build Environ.* (2006) 41:94–108. doi: 10.1016/j.buildenv.2005.01.013
62. Taleghani M, Kleerekoper L, Tenpierik M, van den Dobbelen A. Outdoor thermal comfort within five different urban forms in the Netherlands. *Build Environ.* (2015) 83:65–78. doi: 10.1016/j.buildenv.2014.03.014
63. Garcia-Nevado E, Dupont N, Bugeat A, Beckers B. Benefits of street sun sails to limit building cooling needs in a mediterranean city. *Building Environ.* (2021) 187:107403. doi: 10.1016/j.buildenv.2020.107403
64. Peeters A, Shashua-Bar L, Meir S, Shmulevich RR, Caspi Y, Weyl M, et al. A decision support tool for calculating effective shading in urban streets. *Urban Climate.* (2020) 34:100672. doi: 10.1016/j.uclim.2020.100672
65. Zheng S, Guldmann J-M, Liu Z, Zhao L. Influence of trees on the outdoor thermal environment in subtropical areas: an experimental study in Guangzhou, China. *Sust Cities Soc.* (2018) 42:482–97. doi: 10.1016/j.scs.2018.07.025